PHYSICAL REVIEW B VOLUME 53, NUMBER 8 15 FEBRUARY 1996-II

Hydrostatic pressure dependence of isoelectronic bound excitons in beryllium-doped silicon

Sangsig Kim and Irving P. Herman
Department of Applied Physics and Columbia Radiation Laboratory, Columbia University, New York, New York 10027

Karen L. Moore and Dennis G. Hall
The Institute of Optics, University of Rochester, Rochester, New York 14627

Joze Bevk
AT&T Bell Laboratories, Murray Hill, New Jersey 07974
(Received 31 July 1995)

Photoluminescence (PL) from the recombination of excitons bound to isoelectronic Be_2 dopants in bulk silicon is measured for pressures up to 60 kbar and temperatures down to 9 K. PL from excitons bound to this Be_2 trap is analyzed by using the Hopfield-Thomas-Lynch model, extended to treat more complex isoelectronic dopants, and several different binding potentials. This modified model describes the change in exciton binding energy with pressure determined from the PL spectrum and the loss of PL at and above 60 kbar when short-range potentials are used. The depth of the potential in this model is relatively insensitive to pressure. Coulomb-based models do not explain these observations as well.

I. INTRODUCTION

Isoelectronic impurities generally refer to substitutional species with the same valence-electron structure as the host atoms. While isoelectronic impurities in II-VI and III-V compound semiconductors, such as GaP, are usually substitutional atoms, in silicon these impurities appear to be multiatomic complexes, such as those involving Be, Cu, Li, Tl, S, or Se, and not substitutional (group-IV) atoms. The isoelectronic impurity in silicon doped by Be is a substitutional-interstitial (SI) pair of Be atoms aligned axially along [111].[1–3] The photoluminescence (PL) spectrum of this single trap composed of two Be atoms has features that are similar to that from a pair of traps in single-substitutional-impurity-doped semiconductors, such as GaP doped by N. This Si:Be trap has been shown to be an isoelectronic acceptor.[4,5]

The Be-pair complexes in silicon serve as radiative centers that improve the quantum efficiency of optical emission in this indirect semiconductor.[4] Enhanced PL in Si has also been observed by using other isoelectronic complexes, such as those formed by selenium and sulfur doping, which may involve copper impurities.[6] This article investigates the binding of excitons to Be isoelectronic complex radiative centers in Si, by measuring the PL spectra from Be-doped Si under hydrostatic pressure over a range of temperatures. In an earlier paper we[7] used pressure tuning to demonstrate that two PL features near the phonon replicas of the zero-phonon peak associated with excitons bound to Be_2 likely correspond to the recombination of excitons bound to other Be complexes. This paper concentrates on the zero-phonon PL peak associated with the Be-pair trap.

The Hopfield-Thomas-Lynch (HTL) model is often used to describe the binding of excitons to isoelectronic impurities.[8] For isovalent acceptors, an electron is trapped in a non-Coulomb short-range impurity potential of the isovalent complex. A bound exciton forms through the long-range Coulomb interaction between the trapped electron and a hole. For an isoelectronic donor, a bound exciton forms between a trapped hole and an electron. The details of exciton formation are probably much more complicated than this model suggests. To date, this model has been applied only to single, substitutional atomic impurities, and to pairs of such impurities. The HTL approach is extended here to model exciton binding to the more complex Be_2 trap.

The crystal field (T_d symmetry) splits the energy levels of the isoelectronic exciton states bound to the Be-pair trap in silicon into $J=1$ and $J=2$ levels separated by 2.18 meV (at ambient pressure); this splitting is called the electron-hole exchange energy.[2] These levels are further split by the uniform uniaxial stress, as is seen in Fig. 1. There is a small uniaxial stress on the radiative center, even at ambient pressure [of magnitude ~0.22 kbar (Ref. 2)], due to the axial nature of the Be pair; this leads to a compression of the Be pair and an extension of neighboring Si atoms. When pressure is applied, this uniaxial stress changes because the Si lattice constant changes, even when the pressure is hydrostatic. The five levels of the bound exciton lead to five potential recombination transitions, which are labeled in Fig. 1. In the absence of strain, lines A and A' are fully allowed transitions, line B is a partially allowed transition, and lines

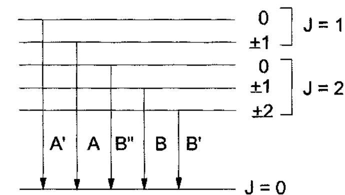

FIG. 1. Diagram of the five energy levels of the isoelectronic exciton split by the crystal field with T_d symmetry and uniform, uniaxial stress; lines A and A' are fully allowed transitions, line B is a partially allowed transition, and lines B' and B'' are forbidden transitions.

 © 1996 The American Physical Society

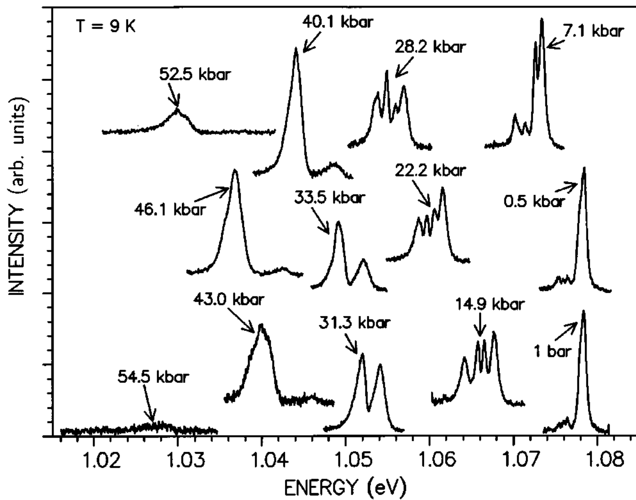

FIG. 2. Zero-phonon PL spectra of Be-doped Si at various pressures (9 K).

B' and B'' are forbidden transitions; uniaxial and biaxial strain-induced mixings make B' and B'' weakly allowed.[9]

At ambient pressure, peak A from the higher-energy feature is dominant at 9 K even though the Boltzmann factor $\exp[-\{E(J=1)-E(J=2)\}/kT]$ is small, 0.06, because the A transition has a much larger oscillator strength than do the B, B', and B'' transitions. Peaks B and B' are dominant at 2 K because this Boltzmann factor is much smaller at this lower temperature, 3×10^{-6}.[9,10] The relative intensities of the zero-phonon lines in the spectra of Si:Be change dramatically with temperature in the range 2–13 K. This trend is generally observed in the luminescence peaks of other semiconductors that are attributable to excitons bound to isoelectronic traps.[10]

II. EXPERIMENTAL PROCEDURE

Be ions were implanted into bulk silicon with a dose of 2×10^{13} ions/cm^2 at 40 keV, as described elsewhere.[4] Measurements were conducted in a diamond anvil cell that was loaded with liquid argon to attain hydrostatic conditions. Pressure uniformity was assessed by measuring PL from two ruby chips placed inside the hole of the gasket along with the thinned sample. Photoluminescence was excited by the 514-nm line from an argon-ion laser (5 mW), which was chopped at 104 Hz. The PL was dispersed by a 0.85-m double spectrometer, detected by a Ge detector, and analyzed by lock-in analysis. Measurements were conducted at 9 K, and at several other higher temperatures, for pressures up to 60 kbar; the PL signal vanished at and above this pressure. After the pressure was released (down to 1 bar), the PL spectrum was found to be the same as that before pressure was applied.

III. RESULTS

Figure 2 shows that as pressure is applied, the PL peaks at 9 K shift toward lower energy, the spectral feature broadens and develops structure, and the relative strengths of the individual PL peaks change dramatically. Qualitatively similar behavior has been observed previously in Si:Be as tempera-

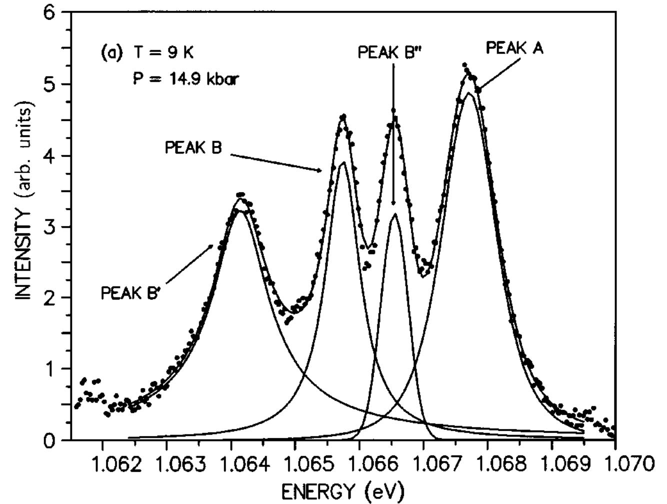

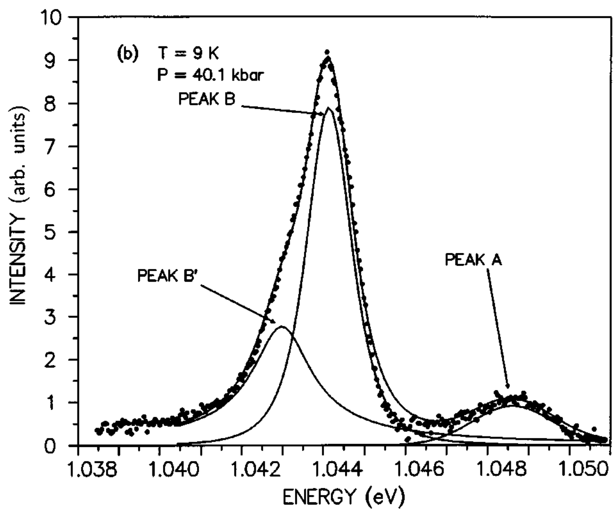

FIG. 3. PL spectra at (a) 14.9 and (b) 40.1 kbar at 9 K fitted by using Pearson VII functions.

ture is changed.[10,11] The four different peaks seen at lower pressures (~7–28 kbar) in Fig. 2 are identified as the A, B, B', and B'' zero-phonon peaks [Fig. 3(a)]; the A' transition is not seen, probably because it is too weakly populated at this temperature. The main peak at 1 bar and 0.5 kbar is the A peak, and the two much smaller peaks seen at lower energies are the B and B' peaks. The new feature seen at a slightly lower energy than the main peak at 7.1 kbar is due to the B'' transition. The energy of this feature agrees with the results of the theoretical work in Ref. 2 and the Zeeman measurements in Ref. 9.

The B, B', and B'' peaks become stronger as pressure is applied. Figure 3(a) shows the resolution of the PL signal at 14.9 kbar (from Fig. 2) into the four observed peaks by using Pearson VII functions,[12] which are peak-fitting functions that can vary between Gaussian and Lorentzian line shapes. Similar fits for each spectrum in Fig. 2 show that the energy differences between the A, B, B', and B'' peaks are constant up to 30 kbar (9 K) within ±0.02 meV, even though the relative strengths of the transitions change greatly.

At higher pressures (Fig. 2), zero-phonon emission has two broader peaks. As resolved in Fig. 3(b), the higher-energy peak is due to the A transition (near 30 kbar this peak

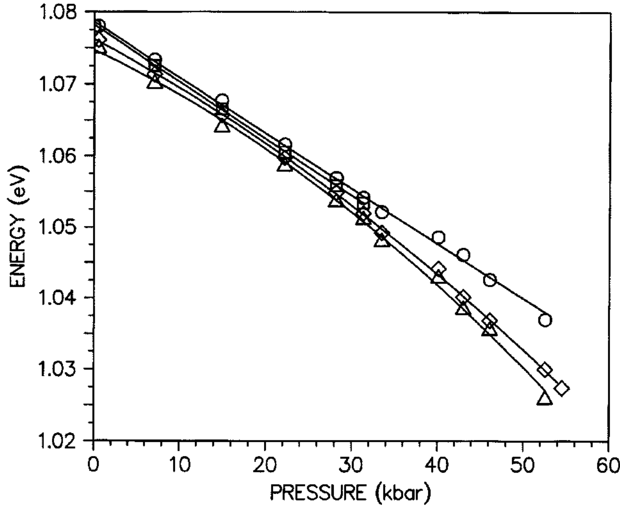

FIG. 4. The dependence of the PL energies of the zero-phonon A (○), B (◇), B' (△), and B'' (□) peaks (from the peak fits) as a function of pressure at 9 K. See Table I for the parameters for the curve fits.

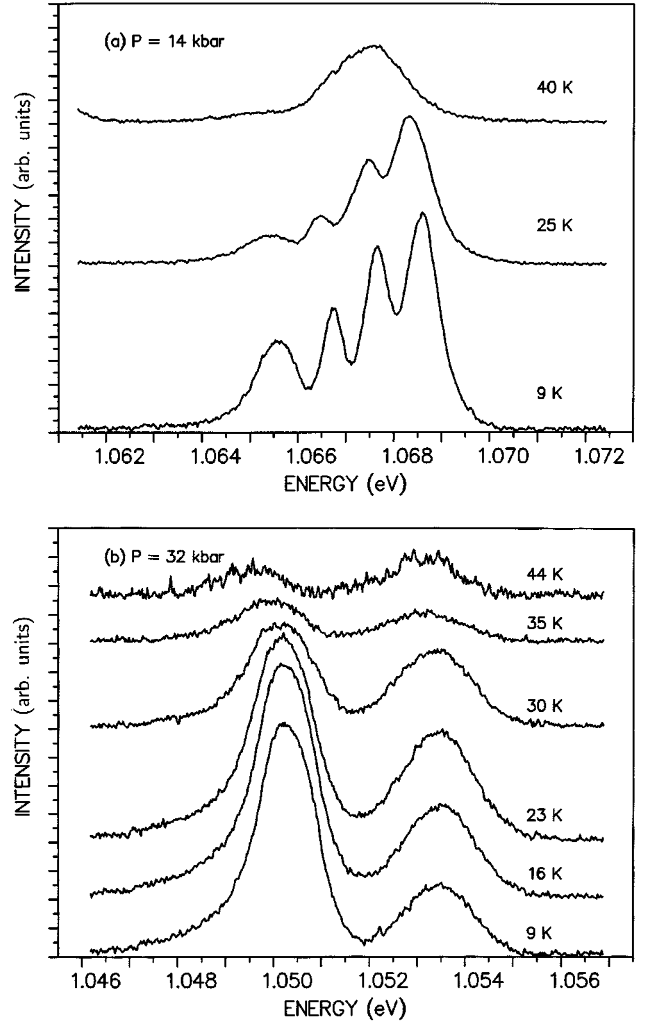

FIG. 5. Zero-phonon PL spectra at (a) 14 and (b) 32 kbar for several temperatures. [The slit width was 0.5 mm, except for the spectrum at 40 K in (a) where it was 1.0 mm. Also, the vertical scale is doubled for the spectrum at 44 K in (b).]

also includes the B'' peak), while the lower-energy peak is due to the B and B' transitions. The PL intensity begins to decrease above ~50 kbar, and no PL is seen above 60 kbar at 9 K.

Figure 4 plots the energies (E) of the A, B, B', and B'' PL peaks, determined from the above-mentioned peak-fitting procedure, as a function of applied pressure (P). The slopes (dE/dP) of these curves are roughly half that of the indirect band gap in Si. The pressure dependences of the four peaks are quite linear up to around 30 kbar and have nearly equal slope, ~0.77 meV/kbar (see Table I). At higher pressures, the pressure dependences of the A and B peaks are different: the energy of peak A decreases more slowly with pressure than that of peak B. Table I presents the fitting parameters for the peak energies of these four zero-phonon peaks, which were obtained with the least-squares fits plotted in Fig. 4.

Figure 5 plots the PL spectra at (a) 14 kbar and (b) 32 kbar, obtained at various temperatures. At 14 kbar, the four peaks merge into a single broader feature and become weaker as the temperature is increased. At 40 K, PL is barely observable. At 32 kbar, two distinct PL peaks are observed at 9 K, which slowly shift to lower energies as the temperature is increased. For both pressures, the integrated intensities of the B, B', and B'' peaks decrease with temperature, while the integrated intensity of the A peak increases up to around 25 K, and then decreases; this is also seen at ambient pressure.[4] The total integrated luminescence is constant up to 25 K, and then decreases rapidly with increased temperature.

TABLE I. Energy positions and pressure coefficients for the four zero-phonon peaks, using the fit $E(P)=E_0(P=1\text{ bar})+\alpha P+\beta P^2$, where P is the pressure in kbar.

Peak	E_0 (1 bar) (eV)	α (meV/kbar)	β (10^{-3} meV/kbar^2)	Fit using data for pressures up to (kbar)
A	1.0783±0.0004	−0.77±0.04	0	52.5
	1.0784±0.0002	−0.76±0.01	0	28.2
B	1.0762±0.0003	−0.63±0.03	−4.9±0.4	54.5
	1.0766±0.0002	−0.77±0.09	0	28.2
B'	1.0747±0.0007	−0.55±0.06	−6.8±0.1	52.5
	1.0754±0.0001	−0.77±0.01	0	28.2
B''	1.0782±0.0001	−0.79±0.01	0	31.3

IV. DISCUSSION

A. General observations

Each of the features associated with the zero-phonon peak decreases with pressure with approximately the same slope, but with a slope that is smaller in magnitude than that of the indirect band gap in Si. As is detailed in Sec. IV B, this is due to the decrease in the binding energy of the exciton with pressure. The slope measured here is roughly equal to the hydrostatic shift rate (0.58±0.06 meV/kbar) estimated in Ref. 2 from uniaxial stress data in the limit of low stress.

In addition to this general behavior, the PL peak has sub-

structure due to the A, B, B', and B'' peaks that changes with pressure, as is seen in Fig. 2. In particular, the relative strengths of these four transitions change greatly as pressure increases. For example, the ratio of the intensities of the B and A peaks is seen to increase from 0.11 at 1 bar to 1.2 at 28.2 kbar to 10 at 46.1 kbar. The PL signal for each peak is proportional to $f_i g_i \exp[-E_i/kT]$, where f_i is the oscillator strength for radiative recombination of the trapped exciton and $g_i \exp[-E_i/kT]$ is the Boltzmann population factor; g_i is the degeneracy of the exciton level i. The change in the ratio of the B and A intensities could be due to variations in the oscillator strengths of these transitions and/or the energy differences of the respective states with pressure.

The energy differences between the A, B, B', and B'' peaks are constant up to 30 kbar (9 K) within ± 0.02 meV, which suggests that in this regime there are no significant changes in the crystal field or uniaxial strain and that the change in the relative peak heights must be due to changes in f_i with pressure. A change in the energy splitting of 0.02 meV would change the ratio of Boltzmann factors only by a factor of 0.97 at 9 K, which is much smaller than the variations observed here.

It is possible that the oscillator strengths of the weaker transitions increase with applied pressure, in part due to uniaxial-strain-induced mixing that is expected even when the applied pressure is hydrostatic. The Be SI pair is compressed along [111] even at ambient pressure, with a uniaxial stress of 0.22 kbar, and the magnitude of strain in the Be pair along [111] should increase as the volume of the Si lattice decreases. (Si and Be have nearly equal bulk moduli.) Reference 2 has calculated that as the uniaxial stress along [111] increases from 0.5 to 2 kbar, the ratio of the oscillator strengths of the B and A transitions increases by a factor of 18. However, concomitantly, the splitting of the A and B peaks would be expected to increase by 7 meV, which is not seen here. Perhaps strain-induced mixing is larger than that calculated or hydrostatic strain changes the level-mixing coefficients.

At pressures above 30 kbar, the energy of peak A decreases at a slightly slower rate than that of peak B, and their splitting increases from 2 meV (the value from 1 bar to 30 kbar) to 7 meV at 50 kbar. According to Ref. 2, an increase in uniaxial stress along [111] increases the energy of peak A and decreases that of peak B; this change in splitting may be due to an increase in the magnitude of uniaxial stress to $\sim$1.75 kbar at 50 kbar. The PL peaks are also observed to broaden with increasing pressure, which may be due to nonuniformities in the strain in the Be SI pair. From 30 to 60 kbar, the two ruby chips gave the same pressure reading within $\sim$0.3 kbar, which suggests this observation is not due to nonhydrostaticity in the applied pressure.

The total integrated luminescence is constant up to 25 K, and then decreases rapidly with increased temperature. As the temperature increases to $\sim$25 K, excitons begin to populate the higher ($J=1$) levels that radiate rapidly and thermal quenching of exciton states is slow; above 25 K nonradiative decay becomes very important. Reference 13 describes several thermal decay modes for excitons, two of which can be important here. For temperatures $>$25 K the hole may escape from the trapped electron. Alternatively, the exciton may decay nonradiatively.

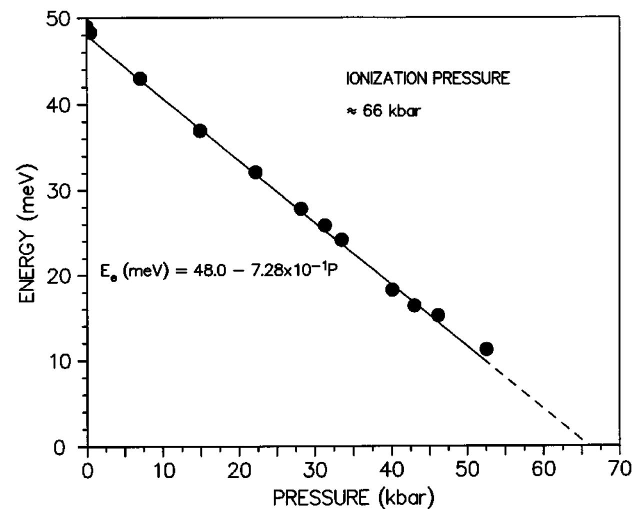

FIG. 6. The binding energy E_e of a trapped electron associated with peak A versus pressure. The solid line fit for E_e (to 52.5 kbar) is extended with the dashed line to the pressure axis to show the intercept. In the inset equation P is the pressure in kbar.

B. Modeling exciton binding

The HTL approach for binding excitons to substitutional atom traps is extended here to model the binding of excitons to the Be SI pairs. An electron is assumed to bind to the isovalent complex and the hole then binds to this electron to form the bound exciton. The overall binding energy (E_{ex}) of a bound exciton relative to the two free particles, given a zero-phonon PL peak at E_{PL} at pressure P, is determined from

$$E_{ex}=1.170 \ \text{eV}-(dE_{BG}/dP)P-E_{PL}, \qquad (1)$$

where 1.170 eV is the indirect band gap (E_{BG}) of Si at 9 K and 1 bar, and $dE_{BG}/dP=1.50$ meV/kbar;[14,15] this assumes that the band gap varies linearly with pressure, which is a satisfactory assumption in this pressure range.[14,16]

From the far-infrared absorption measurements in Ref. 5, the energy required to remove a hole from a trapped electron ($E_{e\text{-}h}$) in this system is 43 meV, which is three times larger than the binding energy of a free exciton in silicon, 14.3 meV.[16] Therefore the binding energy of the trapped electron E_e is

$$E_e=E_{ex}-E_{e\text{-}h}. \qquad (2)$$

It is assumed that the dependence of $E_{e\text{-}h}$ on pressure is negligible; this is justified in Sec. IV B.1. The binding energy of a trapped electron E_e associated with peak A is plotted versus pressure in Fig. 6.

Most detailed theories on the effect of hydrostatic pressure on isoelectronic impurities have concentrated on isolated and paired substitutional traps.[15,17,18] The simple, potential-well model has been used to estimate the binding energies of excitons to a single (neutral) substitutional trap[19] and to pairs of these traps.[20,21] It is not clear whether this approach, and the binding mechanisms assumed, can be applied to Be-pair traps because one of the atoms is interstitial. Further, though the overall Be trap is neutral, each member is

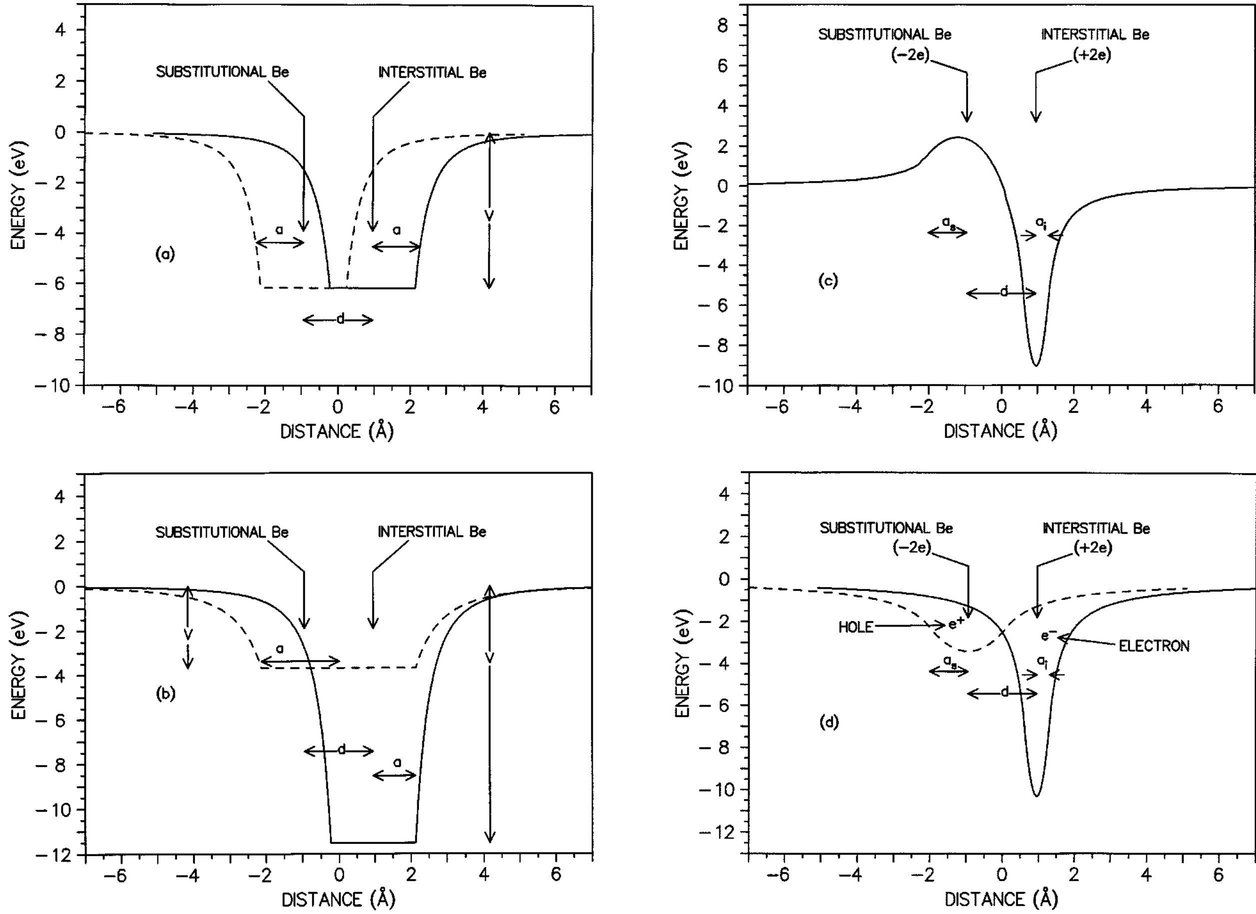

FIG. 7. Four models examined for analyzing the binding mechanism of the isoelectronic exciton bound to the Be SI pair. The double-potential-well model [(a) model A; sum of equivalent potentials about the substitutional Be (dashed lines) and interstitial Be (solid lines)] and the single-potential-well models [(b) model B; potential centered at the interstitial Be (solid lines, model $B1$) or in the middle of the pair (dashed lines, model $B2$)] are not based on Coulomb interactions. In one Coulomb potential model [(c) model C], the Coulomb potential is created additively by both the substitutional Be ion $(-2e)$ and the interstitial Be ion $(+2e)$; this creates both a barrier and well for the electron (and hole, whose potential is the negative of that shown). In another Coulomb potential model [(d) model D], the charge $(+2e)$ of the interstitial Be ion creates a Coulomb potential well for electrons (solid line) and the effect of the other ion is ignored, and the charge $(-2e)$ of the substitutional Be ion creates a well for holes (dashed line) and the effect of the other ion is ignored. $\epsilon=\epsilon_0$ (a constant) is assumed in the potentials depicted in (c) and (d).

probably not. Reference 3 states that the substitutional Be species has charge $-2e$, while the interstitial species has charge $+2e$.

Four different models will be examined, which are illustrated in Fig. 7. In each case the Hamiltonian describing electron binding is

$$H=\left(-\frac{\hbar^2}{2m_e}\right)\nabla^2+V_i(\mathbf{r})+V_s(\mathbf{r}+\mathbf{d}), \tag{3}$$

where V is the potential describing the interaction of an electron with a Be atom. $\mathbf{r}$ is the vector from the interstitial Be atom to the electron and $\mathbf{d}$ is that from the interstitial to substitutional Be atom; their magnitudes are r and d, respectively. The subscripts i and s refer to the interstitial and substitutional Be species, respectively. This equation can also be used to describe the binding of the hole to the trap. The appropriate effective masses of electrons m_e and holes m_h are used.

The Schrödinger equation is solved by the variational method, with a trial function:

$$u(\mathbf{r})=(\gamma^3/\pi)^{1/2}\exp(-\gamma r), \tag{4}$$

where γ is the variational parameter.

1. Models not based on Coulomb interactions

In model A, it is assumed that the interstitial atom creates the same potential well for electrons as does the substitutional atom, and Coulomb interactions are ignored [Fig. 7(a)]. Therefore the same potential is used to bind electrons to each species in the Be pair. A double-potential-well model in the one-band approximation is used, with each equivalent, spherically symmetric well having the form

$$V_j(\mathbf{r})=\begin{cases}-V & (r\leqslant a_j)\\ -V(a_j/r)^3 & (r\geqslant a_j),\end{cases} \tag{5}$$

where V is well depth, and $j=s,i$. This form was used in Refs. 20 and 21 to analyze exciton binding to pairs of neutral

substitutional isovalent atoms. The short-range portion ($r \leqslant a_j$) of this potential is due, in part, to the pseudopotential difference between the bulk and impurity atoms and the long-range portion ($r \geqslant a_j$) is a tail caused by strain effects.[21] The wells for the two Be atoms are separated by a distance d. The hole is assumed to bind to the bound electron by $E_{e\text{-}h}=43$ meV, which is assumed to be independent of pressure.

Following Refs. 20 and 21, the radius of the potential at ambient pressure is set equal to half the nearest-neighbor distance, so $a_0=1.18$ Å. From Ref. 3, the distance between two wells at ambient pressure d_0 is set equal to 1.9 Å, which is the separation that makes the Be SI pair along the [111] direction the most stable. It is assumed that the radius of this potential, a, and the distance between the two Be atoms, d, both change with pressure in a manner proportional to the fractional change in the silicon lattice constant. This gives

$$a=a_0\left(1-\frac{P}{3B}\right), \tag{6a}$$

$$d=d_0\left(1-\frac{P}{3B}\right), \tag{6b}$$

respectively, where the bulk modulus $B=980$ kbar.[22]

Since Eq. (3) is similar to that for the ionized hydrogen molecule, the variational methods used to find the energy levels for H_2^+ are employed here,[23] along with the potential given by $V(\mathbf{r})+V(\mathbf{r}+\mathbf{d})$, using Eq. (5) and the trial wave function given by $\Psi(\mathbf{r})=[u(\mathbf{r}+\mathbf{d})+u(\mathbf{r})]/[2(1+S)]^{1/2}$, where $u(\mathbf{r})$ is given by Eq. (4) and $S=\langle u(\mathbf{r}+\mathbf{d})|u(\mathbf{r})\rangle$.

The binding energy of the trapped electron is obtained by minimizing

$$E_e=(\langle u(\mathbf{r})|H|u(\mathbf{r})\rangle+\langle u(\mathbf{r}+\mathbf{d})|H|u(\mathbf{r})\rangle)/(1+S), \tag{7}$$

which is

$$E_e=-\hbar^2\gamma^2/2m_e+(\hbar^2\gamma^2/m_e+\gamma A+B+2C+D)/(1+S), \tag{8}$$

where

$$S(d)=\langle u(\mathbf{r}+\mathbf{d})|u(\mathbf{r})\rangle=(1+\gamma d+\gamma^2 d^2/3)\exp(-\gamma d), \tag{9}$$

$$A(d)=\langle u(\mathbf{r}+\mathbf{d})|1/r|u(\mathbf{r})\rangle=\gamma(1+\gamma d)\exp(-\gamma d), \tag{10}$$

$$B(a,V)=\langle u(\mathbf{r})|V(\mathbf{r})|u(\mathbf{r})\rangle, \tag{11}$$

$$C(a,d,V)=\langle u(\mathbf{r})|V(\mathbf{r})|u(\mathbf{r}+\mathbf{d})\rangle, \tag{12}$$

$$D(a,d,V)=\langle u(\mathbf{r}+\mathbf{d})|V(\mathbf{r})|u(\mathbf{r}+\mathbf{d})\rangle. \tag{13}$$

a, d, and V are pressure-dependent parameters.

Since the conduction-band edges are not isotropic at the Brillouin zone center but spheroids oriented along the equivalent [100] in the Brillouin zone, the appropriate electron mass is assumed to be the geometric mean of the principal effective masses, $m_e=(m_l m_t^2)^{1/3}=0.32m_0$.[24] The longitudinal effective mass is $m_l=0.92m_0$, the transverse effective mass $m_t=0.19m_0$,[16] and m_0 is the free-electron mass. This choice seems appropriate when the electron states are assumed to be Bloch states at the minimum of the conduction band.[9]

As the pressure is increased, the width of each potential well decreases, which increases the level energy, and the wells move closer together, which decreases the energy. The data in Fig. 6 can be fit very well by using the above-stated pressure dependences of a and d, and a well depth $V=6.167$ eV that is nearly independent of pressure. (There is a very small region where, because of the overlap of the two wells, the potential depth is 12.33 eV. This overlap has only a minor effect on the results.)

The zero-phonon PL peaks disappear around 60 kbar, which means that at these higher pressures either the electron is no longer bound or the hole no longer binds to the trapped electron. The line in Fig. 6 describing the binding energy of a trapped electron E_e vs pressure for peak A extrapolates to zero at the "ionization pressure" of 66 kbar. This is consistent with the prediction of the double-potential-well model with the above fit parameters, which shows that there are bound states for the electron only for pressures below 67 kbar. Since the PL intensity vanishes for pressures approaching ~60 kbar (9 K), this suggests that at these pressures the electron is no longer bound to the trap.

The possibility of electron trapping, and consequently exciton formation, is very sensitive to the depth of the potentials in model A. At ambient pressure, electron binding to the pair trap is possible only for well depths $V>5.831$ eV.

This double-potential-well model suggests that the reduction in the binding energy of the trapped electron can be attributed mostly to the contraction of the dimensions of wells about each Be atom. dV/dP is very small, ~ -0.5 meV/kbar ($[dV/dP]/V=-0.01\%$/kbar) for each potential well of the Be SI pair when the geometric mean of the principal effective masses is used in the model and a and d vary with pressure. If, instead, it is assumed that a and d do not vary with P, then $[dV/dP]/V$ would be -0.08%/kbar, which is still relatively small. In contrast, the depth of the potential well about a simple substitutional isoelectronic impurity appears to depend on pressure more strongly. For example, the PL spectra obtained at different pressures can be fit well only if $[dV/dP]/V=-1.55\%$/kbar for GaAs:N and -0.5%/kbar for GaP:N.[18,20]

Model B assumes a single potential well of the form of Eq. (5) [Fig. 7(b)]. The electron binding energy is $E_e=\langle u(\mathbf{r})|H|u(\mathbf{r})\rangle$, with the trial wave function given by Eq. (4). Two cases are considered here. In model $B1$, there is a single well about only one of the Be atoms, which recognizes that the two Be atoms probably bind the electron differently. Since it is likely that the electron binds to the positively charged interstitial Be species, $V_i(\mathbf{r})$ is given by Eq. (5) and $V_s(\mathbf{r})$ is assumed to be zero. This gives $V=11.513$ eV with $a=1.18$ Å at ambient pressure, which is half the nearest-neighbor Si-Si distance. In model $B2$, a single well represents the overall potential of the electron to the pair of Be atoms, and so it is similar to model A. Model $B2$ fits the data well for $V=3.678$ eV and $a=2.13$ Å; here, $2a$ is the distance between Be atoms (1.9 Å) plus twice the radius of the potential on either side (1.18 Å). Models $B1$ and $B2$ can both be fitted to the data if a is assumed to scale with pressure as

in Eq. 6(a). Again, V is found to be nearly independent of pressure; $[dV/dP]/V=+0.002\%$/kbar for model $B1$ and -0.1%/kbar for model $B2$.

Electrons bind to a single potential well only for $V>11.158$ eV (model $B1$), which is much deeper than the potential depth assumed for the double well in model A. The very large well depth (in each model) may partially explain why excitons in Si often bind to isoelectronic impurity pairs or complexes rather than to single impurities. (The well depths V for GaAs:N and GaP:N are 2.112 and 1.15 eV, respectively.[18,20])

The binding energy of the hole to an electron $E_{e\text{-}h}$ that is bound to a single well can be determined by assuming that the hole interacts only with the Coulomb potential of the electron; details are found in the Appendix. In this calculation the electron wave function obtained in the above variational analysis is used unchanged and the hole wave function is assumed to have the form of Eq. (4), with variational parameter η instead of γ. The effective masses used here are $m_e=0.32m_0$ for the electron and $m_h=0.40m_0$ for the hole,[5] and the dielectric constant for bulk Si $\epsilon_0=11.4$ is used in Coulomb interactions.[25] Since the electron is trapped very near the well, the size of the exciton is determined mostly by the Bohr radius of the hole $1/\eta$. ($1/\gamma=3.2$ Å at 1 bar and 3.4 Å at 50 kbar for model $B1$ and 4.9 Å at 1 bar and 6.0 Å at 50 kbar for model $B2$; for comparison, $1/\gamma=3.4$ Å at 1 bar and 3.8 Å at 50 kbar for model A.) For model $B1$, $E_{e\text{-}h}=36$ meV and $1/\eta=18$ Å and for model $B2$, $E_{e\text{-}h}=32$ meV and $1/\eta=20$ Å, using Eq. (A7). $E_{e\text{-}h}$ and $1/\eta$ are essentially independent of pressure. Both values of $E_{e\text{-}h}$ are smaller than the experimental value, 43 meV. For a perfect acceptor, i.e., assuming the electron radius $1/\gamma=0$ Å, the calculation gives $E_{e\text{-}h}=42$ meV. (Although these calculations were not performed for the more complicated case of model A, $E_{e\text{-}h}$ for model A should be similar to that for model $B2$.)

The experimental value $E_{e\text{-}h}=43$ meV is known to correspond to a perfect acceptor radius of 22 Å when the full 6×6 Hamiltonian (with heavy holes, light holes, and electrons of both spins) is applied.[4,25] Models $B1$ and $B2$ would predict a slightly smaller radius, apparently because the electrons and holes are considered to be decoupled. Therefore any determination of exciton radius here is an underestimate.

As the distance between the electron and hole decreases, eventually becoming shorter than the nearest-neighbor distance, the value of ϵ in the Coulomb potential decreases from the bulk value 11.4 down to 1. Including this screening effect as a spatially dependent dielectric function ϵ in models $B1$ and $B2$, instead of the dielectric constant ϵ_0, should increase $E_{e\text{-}h}$, bringing it closer to the experimental value. (This screening effect is used in Sec. IV B 2.)

The change in $E_{e\text{-}h}$ and η with pressure can be determined by utilizing the changes in the electron wave function with pressure. For both models $B1$ and $B2$, the fractional change in $E_{e\text{-}h}$ is found to be less than 0.1%/kbar and the Bohr radius of the hole is seen to be essentially unchanged with increasing pressure. Similarly, it is safe to assume that $E_{e\text{-}h}$ does not vary with pressure in model A.

Models A, $B1$, and $B2$ each can be used to describe how the binding energy of an exciton bound to the SI Be trap changes with pressure, and each attributes the disappearance of PL above ~60 kbar to the detachment of the electron from the trap.

2. Models based on Coulomb interactions

In models C and D, the charged particles bind to the trap only by Coulomb interactions. It is assumed that the charge of each Be ion is uniformly distributed in a spherical volume, so the Coulomb potential well for either ion is

$$V(r)=\begin{cases} -\dfrac{Ze^2}{\epsilon a_j}\left(\dfrac{3}{2}-\dfrac{1}{2}\dfrac{r^2}{a_j^2}\right) & (r\leqslant a_j)\\ -\dfrac{Ze^2}{\epsilon r} & (r\geqslant a_j),\end{cases} \tag{14}$$

where a_j is the ionic radius of the respective Be atom and ϵ is the dielectric function. The dielectric function $\epsilon(r)$ used here assumes screening:

$$\frac{1}{\epsilon(r)}=\frac{1}{\epsilon_0}+A'e^{-\alpha_1 r}+(1-A')e^{-\alpha_2 r}-\frac{1}{\epsilon_0}e^{-\alpha_3 r}, \tag{15}$$

where the four parameters A', α_1, α_2, and α_3 for Si are given in Ref. 25. For the substitutional Be ion (Be^{2-}), $Z_s=-2$ and $a_s=1.06$ Å,[26] which is also nearly equal to half the Si-Si bond distance (1.18 Å). For the interstitial Be ion (Be^{2+}), $Z_i=+2$ and $a_i=0.35$ Å.[26] The same expression can be used for holes, with appropriate changes in masses and the sign of the potential. The attractive potential of the interstitial Be ion (for electrons) is deeper and more localized than the repulsive potential of the substitutional Be ion. Tarnow *et al.*[3] suggested this as the reason why electrons, and not holes, bind first to the trap.

In model C, the electron interacts with both ions through Eqs. (3) and (14) [Fig. 7(c)]. The trial wave function is Eq. (4) centered at the potential minimum, which is also the position of the interstitial ion. (Even though the Coulomb potential of the Be pair is not spherically symmetric, this trial function should still be satisfactory for examining the existence of the bound states.) With this potential and $\epsilon=\epsilon(r)$ or ϵ_0, the binding energy of the trapped electron $E_e=\langle u(\mathbf{r})|H|u(\mathbf{r})\rangle$ is positive and the electron does not have any bound states about this pair trap; the hole also does not bind to this potential. Moreover, neither electrons nor holes bind to this potential if it is assumed that the ions are pointlike ions ($a_j=0$). This is clear from the binding energy from variational analysis (with $\epsilon=\epsilon_0$):

$$E_e=\frac{\hbar^2\gamma^2}{2m_e}-\frac{2e^2}{\epsilon_0}\left(\gamma-\frac{1-(1+\gamma d)\exp(-2\gamma d)}{d}\right). \tag{16}$$

If instead of these bulklike assumptions for ϵ and m_e, electron binding is assumed to be so tight that it is reasonable to assume that $\epsilon=1$ and $m_e=m_0$ (vacuumlike conditions), then the model C potential leads to very tight electron binding at ambient pressure ($1/\gamma=0.27$ Å, assuming either a_j as above or pointlike charges). However, then the electron binding energy, 39 eV, is much too large. If ϵ and m_e are interpolated between these bulklike and vacuumlike values, then model C gives the ambient pressure E_e for $\epsilon=3.33$ and $m_e=0.85m_0$ ($1/\gamma=1.3$ Å); however, the binding energy is very sensitive to small changes in these parameters, and this model does not seem plausible.

In the single Coulomb potential model D [Fig. 7(d)], the electron is affected only by the attractive potential of the interstitial Be ion (and $V_s=0$). This model can also be used to examine binding of the hole to the trap, by using the attractive potential of the substitutional Be ion (and $V_i=0$). The variational calculation using $\epsilon(r)$ and the effective masses shows that the binding energy of a hole (234 meV) is larger than that of an electron (175 meV); this arises primarily because the mass of the hole is greater than that of the electron. The relatively deep attractive potential for the electron has a much smaller effect on binding than the effective mass. This is clear from first-order perturbation theory, using $\epsilon=\epsilon_0$, for which the binding energy is

$$E_b=Z^2\,\frac{13.6\ \text{eV}}{\epsilon_0^2}\,\frac{m^*}{m_0}\left[1-\frac{4}{5}\left(\frac{a_r}{a_B}\right)^2\right], \tag{17}$$

where a_r is the radius of an ionic Be atom, a_B is the Bohr radius, and m^* is the respective effective mass. (For $\epsilon=\epsilon_0$, both the variational calculation and first-order perturbation theory give 130 and 170 meV as the binding energies for an electron and a hole, respectively.) The "acceptorlike" character of the SI pair cannot be explained by this model.

Neither Coulomb model seems to describe exciton binding well.

V. CONCLUDING REMARKS

The binding of excitons to isoelectronic Be SI pair traps in Si has been described by adapting the HTL model to this isoelectronic dopant and to the conditions of hydrostatic pressure and by using it to examine the PL spectra of Si:Be under pressure. The electrons appear to be bound to the Be pair by an interaction that can be modeled either as a double well or a single well in the one-band approximation, with $1/r^3$ tails. The depths of the wells appear to be relatively independent of pressure. The binding energy of this trapped electron decreases with increased pressure at a rate of 0.73 meV/kbar, assuming that the energy required for separating a hole from a trapped electron is 43 meV. This model explains both the change of exciton energy with pressure and the disappearance of PL above ~60 kbar. Models based on Coulomb interactions between the Be ions and electrons and holes are inconsistent with these observations.

ACKNOWLEDGMENTS

This work was supported at Columbia University (S.K. and I.P.H.) by the Joint Services Electronics Program, Contract No. DAAH04-94-G-0057, and at the University of Rochester (K.L.M. and D.G.H.) by the U. S. Air Force Office of Scientific Research, Contract F49620-92-J-0336. We would also like to thank Professor G. Neumark for valuable discussions.

APPENDIX: CALCULATION OF $E_{e\text{-}h}$

The Hamiltonian for a system composed of a hole interacting with a trapped electron is

$$H=\left(-\frac{\hbar^2}{2m_h}\right)\nabla_h^2+V_{e\text{-}h}(\mathbf{r}_{e\text{-}h}), \tag{A1}$$

where $V_{e\text{-}h}$ is the Coulomb interaction between the electron and hole, and $\mathbf{r}_{e\text{-}h}=\mathbf{r}_e-\mathbf{r}_h$. The wave function of this system is $\psi=u_h(\mathbf{r}_h)u_e(\mathbf{r}_e)$, where $u_h(\mathbf{r}_h)=(\eta^3/\pi)^{1/2}\exp(-\eta r_h)$ and $u_e(\mathbf{r}_e)=(\gamma^3/\pi)^{1/2}\exp(-\gamma r_e)$ are the wave functions for the hole and the electron, respectively. Here η is a variational parameter and γ is already known and is assumed to be unaffected by the interaction with the hole.

Then $E_{e\text{-}h}=\langle\psi|H|\psi\rangle$ or

$$E_{e\text{-}h}(\eta)=\frac{\eta^2\hbar^2}{2m_h}-\frac{e^2\eta^3\gamma^3}{\pi^2\epsilon_0}\int\int\frac{e^{-2\gamma r_e}e^{-2\eta r_h}}{|\mathbf{r}_e-\mathbf{r}_h|}\,d^3r_e d^3r_h. \tag{A2}$$

After letting $\rho_h=2\gamma r_h$ and $\rho_e=2\gamma r_e$, the Coulomb interaction energy between the hole and the trapped electron, $V_{e\text{-}h}$ is

$$V_{e\text{-}h}(\eta)=\frac{e^2\eta^3}{2^5\epsilon_0\pi^2\gamma^2}\int\int\frac{e^{-\rho_e}e^{-(\eta/\gamma)\rho_h}}{|\boldsymbol{\rho}_e-\boldsymbol{\rho}_h|}\,d^3\rho_e d^3\rho_h. \tag{A3}$$

Using the analogy in electrostatics, this expression can be rewritten as

$$V_{e\text{-}h}(\eta)=\frac{e^2\eta^3}{2^5\epsilon_0\pi^2\gamma^2}\int\Phi(\rho_h)e^{-(\eta/\gamma)\rho_h}d^3\rho_h, \tag{A4}$$

where

$$\Phi(\rho_h)=\frac{4\pi}{\rho_h}\int_0^{\rho_h}e^{-\rho_e}\rho_e^2 d\rho_e+4\pi\int_{\rho_h}^{\infty}e^{-\rho_e}\rho_e d\rho_e. \tag{A5}$$

This gives

$$V_{e\text{-}h}(\eta)=\frac{e^2\eta^3}{2\epsilon_0\gamma^2}\int_0^{\infty}[2-e^{-\rho_h}(\rho_h^2+2)]e^{-(\eta/\gamma)\rho_h}d\rho_h. \tag{A6}$$

Using this in Eq. (A2) gives

$$E_{e\text{-}h}(\eta)=\frac{\eta^2\hbar^2}{2m_h}-\frac{e^2\eta^3}{\epsilon_0}\left(\frac{1}{\eta^2}-\frac{3\gamma^2}{(\gamma+\eta)^4}-\frac{1}{(\gamma+\eta)^2}\right). \tag{A7}$$

Using the variational method, this expression is minimized with respect to η to give the hole binding energy and the hole radius. In the limit when the charge distribution of the trapped electron reduces to a point charge, the value of $E_{e\text{-}h}$ is the ionization energy of the perfect acceptor $[13.6(m_h/m_0)/\epsilon_0^2]$ eV. When the Bohr radius of a trapped electron is infinity ($\gamma=0$), Eq. (A7) gives $E_{e\text{-}h}=0$.

[1] R. K. Crouch, J. B. Robertson, and T. E. Gilmer, Jr., Phys. Rev. B **5**, 3111 (1972).

[2] G. Davies, J. Phys. C **17**, 6331 (1984); E. C. Lightowlers and G. Davies, Solid State Commun. **53**, 1055 (1985).

[3] E. Tarnow, S. B. Zhang, K. J. Chang, and D. J. Chadi, Phys. Rev. B **42**, 11 252 (1990).

[4] R. A. Modavis, D. G. Hall, J. Bevk, B. S. Freer, L. C. Feldman, and B. E. Weir, Appl. Phys. Lett. **57**, 954 (1990).

[5] D. Labrie, T. Timusk, and M. L. W. Thewalt, Phys. Rev. Lett. **52**, 81 (1984).

[6] P. L. Bradfield, T. G. Brown, and D. G. Hall, Phys. Rev. B **38**, 3533 (1988); A. M. Frens, M. T. Bennebroek, J. Schmidt, W. M.

Chen, and B. Monemar, *ibid*. **46**, 12 316 (1992); W. M. Chen, M. Singh, B. Monemar, A. Henry, E. Janzén, A. M. Frens, M. T. Bennebroek, and J. Schmidt, *ibid*. **50**, 7365 (1994); E. Sörman, W. M. Chen, A. Henry, S. Andersson, E. Janzén, and B. Monemar, *ibid*. **51**, 2132 (1995).

[7] S. Kim, I. P. Herman, K. L. Moore, D. G. Hall, and J. Bevk, Phys. Rev. B **52**, 16 309 (1995).

[8] J. J. Hopfield, D. G. Thomas, and R. T. Lynch, Phys. Rev. Lett. **17**, 312 (1966).

[9] N. Killoran, D. J. Dunstan, M. O. Henry, E. C. Lightowlers, and B. C. Cavenett, J. Phys. C **15**, 6067 (1982).

[10] M. O. Henry, E. C. Lightowlers, N. Killoran, D. J. Dunstan, and B. C. Cavenett, J. Phys. C **14**, L255 (1981).

[11] M. O. Henry, K. G. McGuigan, M. C. do Carmo, M. H. Nazare, and E. C. Lightowlers, J. Phys. Condens. Matter **2**, 9697 (1990).

[12] J. K. Ord, *Families of Frequency Distributions* (Griffin, London, 1972), p. 101.

[13] M. D. Sturge, E. Cohen, and K. F. Rodgers, Phys. Rev. B **15**, 3169 (1977).

[14] G. A. Northrop, J. F. Morar, D. J. Wolford, and J. A. Bradley, Appl. Phys. Lett. **61**, 192 (1992).

[15] R. D. Hong, D. V. Jenkins, S. Y. Ren, and J. D. Dow, Phys. Rev. B **38**, 12 549 (1988).

[16] *Semiconductors. Physics of Group IV Elements and III-V Compounds*, edited by O. Madelung, Landolt-Börnstein, New Series, Group III, Vol. 17, Pt. a (Springer, Berlin, 1982), p. 43.

[17] J. Shen, S. Y. Ren, and J. D. Dow, Phys. Rev. B **42**, 9119 (1990).

[18] B. Gil, J. P. Albert, J. Camassel, H. Mathieu, and C. Benoit à la Guillaume, Phys. Rev. B **33**, 2701 (1986).

[19] S. H. Sohn and Y. Hamakawa, Phys. Rev. B **46**, 9452 (1992).

[20] B. Gil, M. Baj, J. Camassel, H. Mathieu, C. Benoit à la Guillaume, N. Mestres, and J. Pascual, Phys. Rev. B **29**, 3398 (1984).

[21] F. Thuselt, K. Kreher, and H.-J. Wünshe, Solid State Commun. **36**, 563 (1980).

[22] J. A. Tuchman and I. P. Herman, Phys. Rev. B **45**, 11 929 (1992).

[23] S. Flugge, *Practical Quantum Mechanics* (Springer, Berlin, 1971), p. 113.

[24] R. R. Sharma and S. Rodriguez, Phys. Rev. **153**, 823 (1967).

[25] J. Bernholc and S. T. Pantelides, Phys. Rev. B **10**, 4935 (1977).

[26] W. B. Pearson, *Crystal Chemistry and Physics of Metals and Alloys* (Wiley, New York, 1972).